Expanded Prussian Blue Analogues Incorporating $[Re_6Se_8(CN)_6]^{3-/4-}$ Clusters: Adjusting Porosity via Charge Balance

Miriam V. Bennett, Laurance G. Beauvais, Matthew P. Shores, and Jeffrey R. Long*

Contribution from the Department of Chemistry, University of California, Berkeley, California 94720-1460

Received April 25, 2001

Abstract: Face-capped octahedral $[Re_6Se_8(CN)_6]^{3-/4-}$ clusters are used in place of octahedral $[M(CN)_6]^{3-/4-}$ complexes for the synthesis of microporous Prussian blue type solids with adjustable porosity. The reaction between $[Fe(H_2O)_6]^{3+}$ and $[Re_6Se_8(CN)_6]^{4-}$ in aqueous solution yields, upon heating, $Fe_4[Re_6Se_8(CN)_6]_3 \cdot 36H_2O$ (**4**). A single-crystal X-ray analysis confirms the structure of **4** to be a direct expansion of Prussian blue ($Fe_4[Fe(CN)_6]_3 \cdot 14H_2O$), with $[Re_6Se_8(CN)_6]^{4-}$ clusters connected through octahedral Fe^{3+} ions in a cubic three-dimensional framework. As in Prussian blue, one out of every four hexacyanide units is missing from the structure, creating sizable, water-filled cavities within the neutral framework. Oxidation of $(Bu_4N)_4[Re_6Se_8(CN)_6]$ (**1**) with iodine in methanol produces $(Bu_4N)_3[Re_6Se_8(CN)_6]$ (**2**), which is then metathesized to give the water-soluble salt $Na_3[Re_6Se_8(CN)_6]$ (**3**). Reaction of $[Co(H_2O)_6]^{2+}$ or $[Ni(H_2O)_6]^{2+}$ with **3** in aqueous solution affords $Co_3[Re_6Se_8(CN)_6]_2 \cdot 25H_2O$ (**5**) or $Ni_3[Re_6Se_8(CN)_6]_2 \cdot 33H_2O$ (**6**). Powder X-ray diffraction data show these compounds to adopt structures based on the same cubic framework present in **4**, but with one out of every three cluster hexacyanide units missing as a consequence of charge balance. In contrast, reaction of $[Ga(H_2O)_6]^{3+}$ with **3** gives $Ga[Re_6Se_8(CN)_6] \cdot 6H_2O$ (**7**), wherein charge balance dictates a fully occupied cubic framework enclosing much smaller cavities. The expanded Prussian blue analogues **4**−**7** can be fully dehydrated, and retain their crystallinity with extended heating at 250 °C. Consistent with the trend in the frequency of framework vacancies, dinitrogen sorption isotherms show porosity to increase along the series of representative compounds **7**, $Ga_4[Re_6Se_8(CN)_6]_3 \cdot 38H_2O$, and **6**. Furthermore, all of these phases display a significantly higher sorption capacity and surface area than observed in dehydrated Prussian blue. Despite incorporating paramagnetic $[Re_6Se_8(CN)_6]^{3-}$ clusters, no evidence for magnetic ordering in compound **6** is apparent at temperatures down to 5 K. Reactions related to those employed in preparing compounds **4**−**6**, but carried out at lower pH, produce the isostructural phases $H[cis\text{-}M(H_2O)_2][Re_6Se_8(CN)_6] \cdot 2H_2O$ (M = Fe (**8**), Co (**9**), Ni (**10**)). The crystal structure of **8** reveals a densely packed three-dimensional framework in which $[Re_6Se_8(CN)_6]^{4-}$ clusters are interlinked through a combination of protons and Fe^{3+} ions.

Introduction

The utility of coordination chemistry in synthesizing microporous solids with tailored properties is gradually becoming evident.[1] Coordination solids are produced by simple ligand substitution reactions in which bridging units capable of linking two or more metal centers displace labile ligands on a metal complex, causing growth of an extended framework to propagate in one, two, or three dimensions. If the bridging units and metal centers have well-defined directional bonding preferences, then some modicum of structural predictability can be achieved. For the purpose of obtaining porous frameworks, a typical approach has been to target an expanded version of a known three-dimensional structure by lengthening one of its components.[1a−c,2] This, however, frequently gives rise to a skeletal framework and a structure in which the anticipated void space is filled by one or more identical interpenetrating frameworks.[2b,d−f,h,j,3] In cases where interpenetration is avoided, the expanded framework often is not robust and collapses upon removal of the included guest molecules.[2c,i,k,m] To date, the use of intact cluster precursors in constructing three-dimensional coordination solids

(1) (a) Hoskins, B. F.; Robson, R. *J. Am. Chem. Soc.* **1990**, *112*, 1546. (b) Zaworotko, M. J. *Chem. Soc. Rev.* **1994**, 283. (c) Moore, J. S.; Lee, S. *Chem. Ind.* **1994**, 556. (d) Yaghi, O. M.; Li, G.; Li, H. *Nature* **1995**, *378*, 703. (e) Bowes, C. L.; Ozin, G. A. *Adv. Mater.* **1996**, *8*, 13. (f) Yaghi, O. M.; Li, H.; Davis, C.; Richardson, D.; Groy, T. L. *Acc. Chem. Res.* **1998**, *31*, 474. (g) Kitagawa, S.; Kondo, M. *Bull. Chem. Soc. Jpn.* **1998**, *71*, 1739. (h) Blake, A. J.; Champness, N. R.; Hubberstey, P.; Li, W. S.; Withersby, M. A.; Schroder, M. *Coord. Chem. Rev.* **1999**, *183*, 117. (i) Lin, K.-J. *Angew. Chem., Int. Ed. Engl.* **1999**, *38*, 2730. (j) Seo, J. S.; Whang, D.; Lee, H.; Jun, S. I.; Oh, J.; Jeon, Y. J.; Kim, K. *Nature* **2000**, *404*, 982. (k) Kasai, K.; Aoyagi, M.; Fujita, M. *J. Am. Chem. Soc.* **2000**, *122*, 2140. (l) Noro, S.; Kitagawa, S.; Kondo, M.; Seki, K. *Angew. Chem., Int. Ed.* **2000**, *39*, 2082.

(2) Selected examples: (a) Hoskins, B. F.; Robson, R. *J. Am. Chem. Soc.* **1989**, *111*, 5962. (b) Gable, R. W.; Hoskins, B. F.; Robson, R. *J. Chem. Soc., Chem. Commun.* **1990**, 1677. (c) Abrahams, B. F.; Hoskins, B. F.; Michail, D. M.; Robson, R. *Nature* **1994**, *369*, 727. (d) MacGillivray, L. R.; Subramanian, S.; Zaworotko, M. J. *J. Chem. Soc., Chem. Commun.* **1994**, 1325. (e) Hoskins, B. F.; Robson, R.; Scarlett, N. V. Y. *J. Chem. Soc., Chem. Commun.* **1994**, 2025. (f) Carlucci, L.; Ciani, G.; Proserpio, D. M.; Sironi, A. *J. Chem. Soc., Chem. Commun.* **1994**, 2755. (g) Carlucci, L.; Ciani, G.; Proserpio, D. M.; Sironi, A. *Angew. Chem., Int. Ed. Engl.* **1995**, *34*, 1895. (h) Hirsch, K. A.; Venkataraman, D.; Wilson, S. R.; Moore, J. S.; Lee, S. *J. Chem. Soc., Chem. Commun.* **1995**, 2199. (i) Liu, F.-Q.; Tilley, T. D. *Inorg. Chem.* **1997**, *36*, 5090. (j) Kuroda-Sowa, T.; Horino, T.; Yamamoto, M.; Ohno, Y.; Maekawa, M.; Munakata, M. *Inorg. Chem.* **1997**, *36*, 6382. (k) Kiritis, V.; Michaelides, A.; Skoulika, S.; Golhen, S.; Ouahab, L. *Inorg. Chem.* **1998**, *37*, 3407. (l) Kiang, Y.-H.; Gardner, G. B.; Lee, S.; Xu, Z.; Lobkovsky, E. B. *J. Am. Chem. Soc.* **1999**, *121*, 8204. (m) Dong, Y.-B.; Smith, M. D.; zur Loye, H.-C. *Angew. Chem., Int. Ed.* **2000**, *39*, 4271.

(3) (a) Hirsch, K. A.; Wilson, S. R.; Moore, J. S. *Chem. Eur. J.* **1997**, *3*, 765. (b) Batten, S. R.; Robson, R. *Angew. Chem., Int. Ed. Engl.* **1998**, *37*, 1460.

10.1021/ja0110473 CCC: $20.00 © 2001 American Chemical Society
Published on Web 07/28/2001

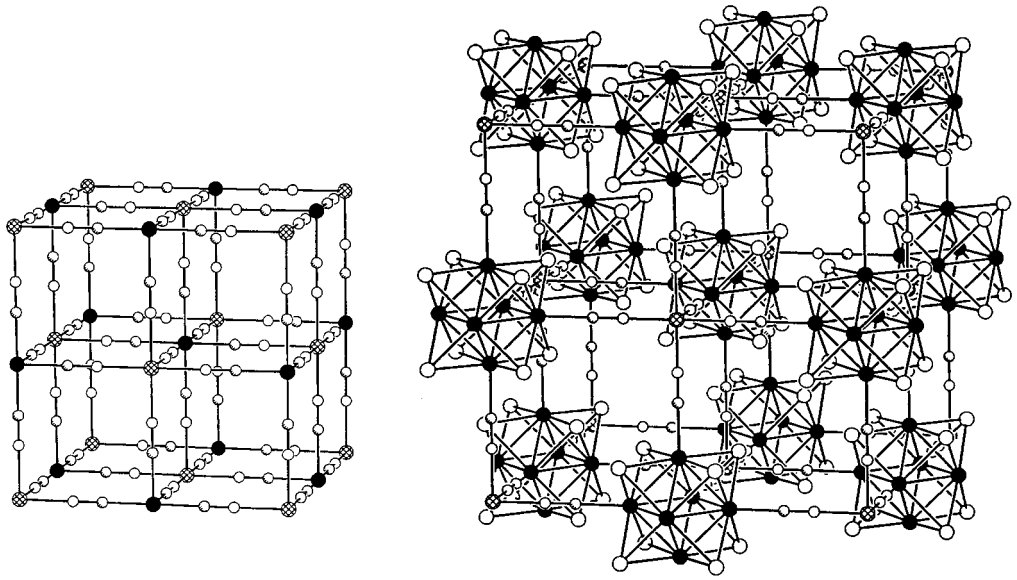

Figure 1. Left: Unit cell for the structure of Prussian blue. Black, shaded, white, and crosshatched spheres represent Fe^{2+}, carbon, nitrogen, and Fe^{3+} centers, respectively. Water molecules have been omitted for clarity, and all $[Fe(CN)_6]^{4-}$ complex sites are only 75% occupied. Right: Unit cell for the structure of a cluster-expanded Prussian blue analogue. Black, large white, crosshatched, shaded, and small white spheres represent Re, Q, M, C, and N atoms, respectively; water molecules have been omitted for clarity.

has been limited.[4−6] In an effort to circumvent the aforementioned difficulties, we have therefore begun to explore the idea of replacing individual metal centers with larger multimetal cluster cores possessing a similar outer coordination geometry.[5] Thus far, our attention has focused on substituting face-capped octahedral clusters of the type $[Re_6Q_8(CN)_6]^{4-}$ (Q = S, Se, Te) for the octahedral $[M(CN)_6]^{4-}$ units in a variety of metal−cyanide frameworks, including that of Prussian blue.[5b]

As one of the oldest known coordination solids, Prussian blue ($Fe_4[Fe(CN)_6]_3 \cdot 14H_2O$) has captivated scientists for nearly three centuries.[7] Its synthesis is readily accomplished by the addition of ferric ions to an aqueous solution containing ferrocyanide ions:

$$4[Fe(H_2O)_6]^{3+} + 3[Fe(CN)_6]^{4-} \rightarrow Fe_4[Fe(CN)_6]_3 \cdot 14H_2O \quad (1)$$

Here, water molecules coordinated to the ferric ions are displaced by nitrogen atoms from the ferrocyanide ions to generate linear $Fe^{II}-CN-Fe^{III}$ bridges and an extended framework based on the face-centered cubic unit cell displayed at the left in Figure 1.[8] Significantly, to achieve charge neutrality, the Prussian blue framework is not precisely that depicted, but rather exhibits a vacancy of 25% of the $[Fe(CN)_6]^{4-}$ units. While the arrangement of these vacancies is typically disordered over long range, crystals produced under slow growth conditions sometimes exhibit regions of primitive cubic ordering.[8b] In either instance, the vacancies result in a much more porous framework wherein, *on average*, the cavities are defined by the cage obtained upon removing the central $[Fe(CN)_6]^{4-}$ moiety from the unit cell in Figure 1. Each such cavity is filled with 14 water molecules, 6 of which bind the exposed Fe^{III} centers. By employing $[Re_6Te_8(CN)_6]^{4-}$ in place of $[Fe(CN)_6]^{4-}$ in reaction 1, we have synthesized the expanded Prussian blue analogue $Fe_4[Re_6Te_8(CN)_6]_3 \cdot 27H_2O$ bearing a directly analogous cubic framework based on the larger unit cell shown at the right in Figure 1.[5b] This expansion leads to a dramatic increase in pore size (again enhanced by the framework vacancies), without inducing interpenetration or loss of framework stability.

When confronted with cyanide or isocyanide as a ligand, a wide selection of metal ions prefer to adopt an octahedral coordination geometry. Consequently, reactions related to reaction 1 above can be used to produce a large family of solids with structures based on the cubic Prussian blue framework (Figure 1, left).[7,9] As precipitated from aqueous solutions containing no extraneous alkali metal salts, these Prussian blue analogues tend to possess neutral frameworks in which charge balance dictates the number of lattice vacancies. For example,

(4) (a) Yaghi, O. M.; Sun, Z.; Richardson, D. A.; Groy, T. L. *J. Am. Chem. Soc.* **1994**, *116*, 807. (b) Naumov, N. G.; Virovets, A. V.; Sokolov, M. N.; Artemkina, S. B.; Fedorov, V. E. *Angew. Chem., Int. Ed. Engl.* **1998**, *37*, 1943. (c) MacLachlan, M. J.; Coombs, N.; Bedard, R. L.; White, S.; Thompson, L. K.; Ozin, G. A. *J. Am. Chem. Soc.* **1999**, *121*, 12005. (d) Naumov, N. G.; Virovets, A. V.; Fedorov, V. E. *Inorg. Chem. Commun.* **2000**, *3*, 71. (e) Fedin, V.; Virovets, A. V.; Kalinina, I. V.; Ikorskii, V. N.; Elsegood, M. R. J.; Clegg, W. *Eur. J. Inorg. Chem.* **2000**, 2341. (f) Rangan, K. K.; Trikalitis, P. N.; Kanatzidis, M. G. *J. Am. Chem. Soc.* **2000**, *122*, 10230.

(5) (a) Beauvais, L. G.; Shores, M. P.; Long, J. R. *Chem. Mater.* **1998**, *10*, 3783. (b) Shores, M. P.; Beauvais, L. G.; Long, J. R. *J. Am. Chem. Soc.* **1999**, *121*, 775. (c) Shores, M. P.; Beauvais, L. G.; Long, J. R. *Inorg. Chem.* **1999**, *38*, 1648. (d) Beauvais L. G.; Shores, M. P.; Long, J. R. *J. Am. Chem. Soc.* **2000**, *122*, 775. (e) Bennett, M. V.; Shores, M. P.; Beauvais, L. G.; Long, J. R. *J. Am. Chem. Soc.* **2000**, *122*, 6663.

(6) There do, however, exist numerous examples of such solids with frameworks featuring cluster components that have been assembled in situ. Selected examples:[1e,f,i] (a) Dance, I. G.; Garbutt, R. G.; Craig, D. C.; Scudder, M. L. *Inorg. Chem.* **1987**, *26*, 4057. (b) Tan, K.; Darovsky, A.; Parise, J. B. *J. Am. Chem. Soc.* **1995**, *117*, 7039. (c) Bowes, C. L.; Huynh, W. U.; Kirkby, S. J.; Malek, A.; Ozin, G. A.; Petrov, S.; Twardowski, M.; Young, D.; Bedard, R. L.; Broach, R. *Chem. Mater.* **1996**, *8*, 2147. (d) Yaghi, O. M. *J. Am. Chem. Soc.* **1997**, *119*, 2861. (e) Khan, M. I.; Yohannes, E.; Powell, D. *Inorg. Chem.* **1999**, *38*, 212. (f) Chui, S. S.-Y.; Lo, S. M.-F.; Charmant, J. P. H.; Orpen, A. G.; Williams, I. D. *Science* **1999**, *283*, 1148. (g) Müller, A.; Krickemeyer, E.; Bögge, H.; Schmidtmann, M.; Beugholt, C.; Das, S. K.; Peters, F. *Chem. Eur. J.* **1999**, *5*, 1496. (h) Khan, M. I.; Yohannes, E.; Doedens, R. J. *Angew. Chem., Int. Ed. Engl.* **1999**, *38*, 1292. (i) Li, H.; Eddaoudi, M.; O'Keeffe, M.; Yaghi, O. M. *Nature* **1999**, *402*, 276.

(7) (a) Ludi, A.; Güdel, H. U. *Struct. Bond.* **1973**, *14*, 1. (b) Dunbar, K. R.; Heintz, R. A. *Prog. Inorg. Chem.* **1997**, *45*, 283 and references therein.

(8) (a) Buser, H. J.; Ludi, A.; Petter, W.; Schwarzenbach, D. *J. Chem. Soc., Chem. Commun.* **1972**, 1299. (b) Buser, H. J.; Schwarzenbach, D.; Petter, W.; Ludi, A. *Inorg. Chem.* **1977**, *16*, 2704.

(9) (a) Weiser, H. B.; Milligan, O.; Bates, J. B. *J. Phys. Chem.* **1942**, *46*, 99. (b) Seifer, G. B. *Russ. J. Inorg. Chem.* **1959**, *4*, 841. (c) Shriver, D. F.; Shriver, S. A.; Anderson, S. E. *Inorg. Chem.* **1965**, *4*, 725.

reactions between trications and trianionic hexacyanometalates generate frameworks with a 1:1 stoichiometry in which the cubic lattice displayed in Figure 1 is fully occupied:

$$[M(H_2O)_6]^{3+} + [M'(CN)_6]^{3-} \rightarrow M[M'(CN)_6]\cdot xH_2O \quad (2)$$

Known compounds of this type include $M[Fe(CN)_6]\cdot xH_2O$ (M = Fe, Ga, In)[10] and $Fe[M'(CN)_6]\cdot xH_2O$ (M′ = Co, Rh, Ir).[11] In contrast, reactions between dications and trianionic hexacyanometalates generate frameworks with a 3:2 stoichiometry and a higher concentration of vacancies than in Prussian blue:

$$3[M(H_2O)_6]^{2+} + 2[M'(CN)_6]^{3-} \rightarrow M_3[M'(CN)_6]_2\cdot xH_2O \quad (3)$$

In such cases, one-third of all hexacyanometalate units are missing from the unit cell depicted at the left in Figure 1, and again the vacancies are disordered over long range. Numerous compounds of this type have been identified, including $M_3[Cr(CN)_6]_2\cdot xH_2O$ (M = Cr, Fe, Co, Cd),[12] $M_3[Mn(CN)_6]_2\cdot xH_2O$ (M = Mn, Fe),[12e,13] $M_3[Fe(CN)_6]_2\cdot xH_2O$ (M = Co, Ni, Cu, Zn, Cd),[13,14] and $M_3[Co(CN)_6]_2\cdot xH_2O$ (M = Mn, Fe, Co, Zn, Cd),[15] where the value of x generally falls within the range 12−15. Thus, the porosity of the metal−cyanide framework in Prussian blue analogues, which directly correlates with the concentration of hexacyanometalate vacancies, is readily manipulated via charge balance.

Herein, we demonstrate an extension of this principle by substituting oxidized $[Re_6Se_8(CN)_6]^{3-}$ clusters for the $[M'(CN)_6]^{3-}$ ions in reactions 2 and 3 to create a family of expanded Prussian blue analogues with adjustable porosity.

Experimental Section

Preparation of Compounds. The compounds $NaCs_3[Re_6Se_8(CN)_6]$,[5a] $Na_4[Re_6Se_8(CN)_6]$,[5b,16] $Ga_4[Re_6Se_8(CN)_6]_3\cdot 38H_2O$,[5b] and $Fe_4[Fe(CN)_6]_3\cdot 14H_2O$[7] were prepared as described previously. $Co_3[Fe(CN)_6]_2\cdot 13H_2O$ and $Ni_3[Fe(CN)_6]_2\cdot 14H_2O$ were also prepared according to previous reports;[14b,d] however, the water content of each of these compounds was reassessed. Water was distilled and deionized with a Milli-Q filtering system. All other reagents were used as purchased. Product identity and purity were verified by comparison of the observed powder X-ray diffraction pattern with a simulated pattern. The water content of each compound was determined by combining results from thermogravimetric and elemental analyses.

$(Bu_4N)_4[Re_6Se_8(CN)_6]$ (1). A solution of Bu_4NBr (3.0 g, 9.3 mmol) in 50 mL of water was added to a solution of $NaCs_3[Re_6Se_8(CN)_6]$ (2.5 g, 1.3 mmol) in 75 mL of water. The resulting orange suspension was stirred and heated at 35 °C for 30 min. The orange solid was collected by filtration, washed with water (3 × 50 mL), and dissolved in a minimal amount of methanol. Diffusing ethyl acetate into this solution produced red rectangular plate-shaped crystals, which were collected by filtration and dried in air at 70 °C to give 2.5 g (67%) of product. IR: ν_{CN} 2106 cm^{-1}. Anal. Calcd for $C_{70}H_{144}N_{10}Re_6Se_8$: C, 29.25; H, 5.05; N, 4.87. Found: C, 29.28; H, 5.00; N, 4.83.

$(Bu_4N)_3[Re_6Se_8(CN)_6]$ (2). A solution of iodine (1.0 g, 4.3 mmol) in 100 mL of methanol was added to a solution of **1** (1.5 g, 0.52 mmol) in 300 mL of methanol, and the mixture was stirred for 5 h at 35 °C. The solution volume was reduced to 80 mL in vacuo, and 300 mL of diethyl ether was added to afford a green precipitate. The solid was collected by filtration and washed with diethyl ether until the filtrate was colorless. It was then recrystallized by diffusing ethyl acetate vapor into a saturated methanol solution. The resulting red-green dichroic crystals were collected by filtration and dried in air to give 0.96 g (70%) of product. IR: ν_{CN} 2123 cm^{-1}. μ_{eff} = 2.08 μ_B at 295 K. Anal. Calcd for $C_{54}H_{108}N_9Re_6Se_8$: C, 24.64; H, 4.14; N, 4.79. Found: C, 24.15; H, 4.14; N, 4.66.

$Na_3[Re_6Se_8(CN)_6]\cdot 3H_2O$ (3). A solution of $NaClO_4$ (0.30 g, 0.15 mmol) in 50 mL of acetonitrile was added to a solution of **2** (1.97 g, 0.75 mmol) in 200 mL of acetonitrile, inducing formation of a green precipitate. The solid was collected by filtration, washed with acetonitrile (3 × 50 mL), and dried under vacuum to give 1.2 g (81%) of product. IR: ν_{CN} 2128 cm^{-1}. Anal. Calcd for $C_6H_6N_6Na_3O_3Re_6Se_8$: C, 3.55; H, 0.30; N, 4.14. Found: C, 3.80; H, 0.31; N, 3.98.

$Fe_4[Re_6Se_8(CN)_6]_3\cdot 36H_2O$ (4). A solution of $Fe(NO_3)_3\cdot 9H_2O$ (0.057 g, 0.14 mmol) in 5 mL of water was acidified to a pH of approximately 1.5 by addition of 6 drops of 45% HNO_3 and then heated for 5 min at 75 °C. A solution of $Na_4[Re_6Se_8(CN)_6]$ (0.060 g, 0.030 mmol) in 5 mL of water was acidified to a pH of approximately 3 by addition of 1 drop of 45% HNO_3 and then also heated for 5 min at 75 °C. Combining the solutions prompted the immediate formation of a black suspension, which was then heated at 75 °C for 12 h. The mother liquor was decanted, and the resulting brown powder was washed with successive aliquots of water (3 × 5 mL) and dried in air to give 0.054 g (80%) of product. IR: ν_{CN} 2135 (broad) cm^{-1}. μ_{eff} = 12.11 μ_B at 295 K. Anal. Calcd for $C_{18}H_{72}Fe_4N_{18}O_{36}Re_{18}Se_{24}$: C, 3.03; H, 1.02; N, 3.53. Found: C, 3.26; H, 1.02; N, 3.49. Black square prism-shaped crystals suitable for X-ray analysis were obtained from a reaction performed at room temperature without added acid by allowing the black solid product to stand under the mother liquor for ca. 2 months.

$Co_3[Re_6Se_8(CN)_6]_2\cdot 25H_2O$ (5). A solution of $Co(NO_3)_2\cdot 6H_2O$ (0.67 g, 2.3 mmol) in 2 mL of water and a solution of **3** (0.062 g, 0.031 mmol) in 2 mL of water were heated separately in an oil bath at 80 °C for 5 min. The solutions were combined to give a green suspension, and the temperature of the oil bath was immediately lowered to 70 °C. After 20 min of heating, the green solid was collected by centrifugation, washed with successive aliquots of water (3 × 5 mL), and dried in air to give 0.046 g (69%) of product. IR: ν_{CN} 2155 (broad) cm^{-1}. μ_{eff} = 8.62 μ_B at 295 K. Anal. Calcd for $C_{12}H_{50}Co_3N_{12}O_{25}Re_{12}Se_{16}$: C, 3.24; H, 1.18; N, 3.78. Found: C, 3.26; H, 1.20; N, 3.77. X-ray powder diffraction showed this compound to be isostructural to **6** with a unit cell parameter of a = 14.008(8) Å.

$Ni_3[Re_6Se_8(CN)_6]_2\cdot 33H_2O$ (6). At room temperature, a solution of $Ni(ClO_4)_2\cdot 6H_2O$ (0.68 g, 1.9 mmol) in 2 mL of water was added to a solution of **3** (0.060 g, 0.030 mmol) in 2 mL of water to afford a green suspension. The reaction mixture was then heated at 75 °C for 12 h. The resulting green solid was collected by centrifugation, washed with successive aliquots of water (3 × 5 mL), and dried in air to give 0.058 g (84%) of product. IR: ν_{CN} 2167 (broad) cm^{-1}. μ_{eff} = 6.12 μ_B at 295 K. Anal. Calcd for $C_{12}H_{66}N_{12}Ni_3O_{33}Re_{12}Se_{16}$: C, 3.15; H, 1.45; N, 3.67; Ni, 3.85; Re, 48.78. Found: C, 3.20; H, 1.37; N, 3.58; Ni, 4.10; Re, 48.80.

$Ga[Re_6Se_8(CN)_6]\cdot 6H_2O$ (7). A solution of $Ga(NO_3)_3\cdot 6H_2O$ (0.060 g, 0.16 mmol) in 2 mL of water was heated at reflux for 10 min. A solution of **3** (0.060 g, 0.030 mmol) in 2 mL of water was acidified to

(10) (a) De Wet, J. F.; Rolle, R. *Z. Anorg. Allg. Chem.* **1965**, *336*, 96. (b) Walker, R. G.; Watkins, K. O. *Inorg. Chem.* **1968**, *7*, 885. (c) Ben-Bassat, A. H. I. *Isr. J. Chem.* **1968**, *6*, 91. (d) Kishore, D.; Gupta, G. P.; Lal, K. C.; Srivastava, T. N. *Z. Phys. Chem. (Wiesbaden)* **1981**, *126*, 127.

(11) Inoue, H.; Fluck, E.; Yanagisawa, S. *Z. Naturforsch.* **1976**, *B31*, 167.

(12) (a) Brown, D. B.; Shriver, D. F. *Inorg. Chem.* **1969**, *8*, 37. (b) Güdel, H.-U. *Acta Chem. Scand.* **1972**, *26*, 2169. (c) Milligan, W. O.; Mullica, D. F.; Hills, F. W. *J. Inorg. Nucl. Chem.* **1981**, *43*, 3119. (d) Mallah, T.; Thiébaut, S.; Verdaguer, M.; Veillet, P. *Science* **1993**, *262*, 1554. (e) Reguera, E.; Yee-Madeira, H.; Fernández-Bertran, J.; Nuñez, L. *Transition Met. Chem.* **1999**, *24*, 163.

(13) Ziegler, B.; Witzel, M.; Schwarten, M.; Babel, D. *Z. Naturforsch.* **1999**, *B54*, 870.

(14) (a) Gravereau, P.; Garnier, E. *Acta Crystallogr.* **1984**, *C40*, 1306. (b) Shyu, H. L.; Lin, S. N.; Wei, H. H. *J. Chin. Chem. Soc.* **1995**, *42*, 791. (c) Ayrault, S.; Loos-Neskovic, C.; Fedoroff, M.; Garnier, E.; Jones, D. J. *Talanta* **1995**, *42*, 1581. (d) Yamada, S.; Kuwabara, K.; Koumoto, K. *Mater. Sci. Eng.* **1997**, *B49*, 89.

(15) (a) Ludi, A.; Güdel, H. U. *Helv. Chim. Acta* **1968**, *51*, 2006. (b) Ludi, A.; Güdel, H.-U.; Rüegg, M. *Inorg. Chem.* **1970**, *9*, 2224. (c) Mullica, D. F.; Milligan, W. O.; Beall, G. W.; Reeves, W. L. *Acta Crystallogr.* **1978**, *B34*, 3558. (d) Mullica, D. F.; Oliver, J. D.; Milligan, W. O.; Hills, F. W. *Inorg. Nucl. Chem. Lett.* **1979**, *15*, 361.

(16) Mironov, Y. V.; Cody, J. A.; Albrecht-Schmitt, T. E.; Ibers, J. A. *J. Am. Chem. Soc.* **1997**, *119*, 493.

Table 1. Crystallographic Data and Structure Refinement Parameters for $(Bu_4N)_3[Re_6Se_8(CN)_6]\cdot 3H_2O$ (**2**·$3H_2O$), $Fe_4[Re_6Se_8(CN)_6]_3\cdot 36H_2O$ (**4**), $Ni_3[Re_6Se_8(CN)_6]_2\cdot 33H_2O$ (**6**), $Ga[Re_6Se_8(CN)_6]\cdot 6H_2O$ (**7**), and $H[cis\text{-}Fe(H_2O)_2][Re_6Se_8(CN)_6]\cdot 2H_2O$ (**8**)

	2·$3H_2O$[a]	**4**[a]	**6**[b]	**7**[c]	**8**[a]
formula	$C_{54}H_{114}N_9O_3Re_6Se_8$	$C_{18}H_{72}N_{18}Fe_4O_{36}Re_{18}Se_{24}$	$C_{12}H_{66}N_{12}Ni_3O_{33}Re_{12}Se_{16}$	$C_6H_{12}GaN_6O_6Re_6Se_8$	$C_6H_9FeN_6O_4Re_6Se_8$
formula wt	2734.50	6298.72	4580.60	2082.80	2033.92
T, K	165	174	295	295	157
space group	*C*2/*m*	$Fm\bar{3}m$	$Fm\bar{3}m$	$Fm\bar{3}m$	$P3_121$
Z	2	1	$1.\bar{3}$	4	3
a, Å	15.5294(9)	14.2455(10)	14.2364(2)	14.1303(1)	12.7255(10)
b, Å	20.5554(11)				
c, Å	13.9577(7)				13.694(2)
β, deg	91.620(2)				
V, Å^3	4453.7(4)	2890.9(4)	2885.36(7)	2821.30(4)	1920.6(3)
μ, mm^{-1}	11.424	26.842			40.190
d_{calc}, g/cm^3	1.972	3.784	3.472	4.903	5.276
R_1, wR_2,[d] %	6.47, 16.16	2.52, 6.98			3.53, 4.70
R_p, wR_p, R_{F2},[e] %			2.80, 3.88, 8.81	3.60, 5.40, 7.19	

[a] Obtained using graphite monochromated Mo Kα ($\lambda = 0.71073$ Å) radiation. [b] Obtained using synchrotron radiation of wavelength $\lambda = 1.27727$ Å. [c] Obtained using synchrotron radiation of wavelength $\lambda = 1.28077$ Å. [d] $R_1 = \sum||F_o| - |F_c||/\sum|F_o|$; $wR_2 = \{[\sum[w(|F_o| - |F_c|)]^2/\sum[w(|F_o|^2)]\}^{1/2}$. [e] $R_p = \sum|y_i(\text{obs}) - y_i(\text{calc})|/\sum y_i(\text{obs})$; $wR_p = \{[\sum[w_i(y_i(\text{obs}) - y_i(\text{calc}))]^2/\sum[w_i(y_i(\text{obs}))^2]\}^{1/2}$; $R_{F2} = \sum|F_o^2 - F_c^2|/\sum F_o^2$.

a pH of approximately 1.5 by addition of 2 drops of 45% $HClO_4$ and then heated at 80 °C for 5 min. These solutions were combined to give a green suspension, which was then heated at 80 °C for 30 min. Upon cooling, the resulting green solid was collected by centrifugation, washed with successive aliquots of water (3 × 5 mL), and dried in air to give 0.042 g (67%) of product. IR: ν_{CN} 2192 (broad) cm^{-1}. $\mu_{eff} = 1.92\ \mu_B$ at 295 K. Anal. Calcd for $C_6H_{12}GaN_6O_6Re_6Se_8$: C, 3.46; H, 0.58; Ga, 3.35; N, 4.03; Na, 0.000. Found: C, 3.15; H, 0.56; Ga, 3.83; N, 4.06; Na, 0.027.

H[*cis*-Fe(H$_2$O)$_2$][Re$_6$Se$_8$(CN)$_6$]·2H$_2$O (8). A solution of $Na_4[Re_6Se_8(CN)_6]$ (0.060 g, 0.030 mmol) in 3 mL of water was acidified to a pH of approximately 1.5 by addition of 3 drops of concentrated H_2SO_4 and then heated at 75 °C for 5 min. A solution of $Fe(NO_3)_3\cdot 9H_2O$ (0.020 g, 0.050 mmol) in 7 mL of water was acidified to a pH of approximately 1.5 by addition of 7 drops of concentrated H_2SO_4 and then also heated at 75 °C for 5 min. These solutions were combined and further heated at 75 °C for 3 h, gradually resulting in formation of a black powder along with black rectangular block-shaped crystals. The pale green supernatant solution was decanted, and the black solid was washed with successive aliquots of water (3 × 10 mL) and dried in air to give 0.046 g (75%) of product. IR: ν_{CN} 2151, 2113 cm^{-1}. $\mu_{eff} = 6.03\ \mu_B$ at 295 K. Anal. Calcd for $C_6H_9FeN_6O_4Re_6Se_8$: C, 3.54; H, 0.45; N, 4.13. Found: C, 3.43; H, 0.54; N, 3.87.

H[*cis*-Co(H$_2$O)$_2$][Re$_6$Se$_8$(CN)$_6$]·2H$_2$O (9). A solution of **3** (0.060 g, 0.030 mmol) in 2 mL of water was acidified to a pH of approximately 1 by addition of 5 drops of concentrated HCl and then heated at 80 °C for 5 min. A solution of $CoCl_2\cdot 6H_2O$ (0.017 g, 0.046 mmol) in 2 mL of water was heated at 80 °C for 5 min. Combining these solutions prompted the immediate formation of a green suspension, which was then heated at 80 °C for 15 min. Upon cooling, the resulting green solid was collected by centrifugation, washed with successive aliquots of water (3 × 5 mL), and dried in air to give 0.055 g (89%) of product. IR: ν_{CN} 2166 (sh), 2144 cm^{-1}. $\mu_{eff} = 5.75\ \mu_B$ at 295 K. Anal. Calcd for $C_6H_9CoN_6O_4Re_6Se_8$: C, 3.54; H, 0.45; N, 3.80. Found: C, 3.35; H, 0.65; N, 4.13. X-ray powder diffraction showed this compound to be isostructural to **8** with the unit cell parameters $a = 12.690(1)$ Å and $b = 13.724(2)$ Å.

H[*cis*-Ni(H$_2$O)$_2$][Re$_6$Se$_8$(CN)$_6$]·2H$_2$O (10). A solution of **3** (0.057 g, 0.028 mmol) in 7 mL of water was acidified to a pH of approximately 1.5 by addition of 7 drops of concentrated H_2SO_4 and then heated at 60 °C for 5 min. A solution of $NiSO_4\cdot 6H_2O$ (0.020 g, 0.076 mmol) in 3 mL of water was acidified to a pH of approximately 1.5 by addition of 3 drops of concentrated H_2SO_4. Combining these solutions immediately induced formation of a green suspension, which was further heated at 60 °C. Upon cooling, the supernatant solution was decanted, and the resulting green solid was washed with successive aliquots of H_2O (3 × 20 mL) and dried in air to give 0.048 g (81%) of product. IR: ν_{CN} 2147 cm^{-1}. $\mu_{eff} = 3.63\ \mu_B$ at 295 K. Anal. Calcd for $C_6H_9N_6NiO_4Re_6Se_8$: C, 3.54; H, 0.45; N, 4.13. Found: C, 3.25; H, 0.54; N, 3.95. X-ray powder diffraction showed this compound to be isostructural to **8** with the unit cell parameters $a = 12.6829(5)$ Å and $b = 13.6694(9)$ Å.

X-ray Structure Determinations. Single crystals of **2**·$3H_2O$, **4**, and **8** were coated in Paratone-N oil, attached to quartz fibers, transferred to a Bruker SMART diffractometer, and cooled in a dinitrogen stream. Lattice parameters were initially determined from a least-squares refinement of more than 38 carefully centered reflections. The raw intensity data were converted (including corrections for background and Lorentz and polarization effects) to structure factor amplitudes and their esd's using the SAINT 5.00 program. An empirical absorption correction was applied to each data set using SADABS. Space group assignments were based on systematic absences, *E*-statistics, and successful refinement of the structures. Structures were solved by direct methods, with the aid of difference Fourier maps, and were refined with successive full-matrix least-squares cycles. One tetrabutylammonium cation and one solvate water molecule in the structure of **2**·$3H_2O$ are disordered over multiple positions, as are all of the solvate water molecules in the structure of compound **4**. Disordered atoms were modeled with partial occupancies. Because of the excessive disorder and high symmetry, the water content in the structure of **4** could not be reliably determined, and was assumed to agree with that established for the bulk solid. Hydrogen atoms were not included in any of the refinements. All other light atoms ($Z < 9$) were refined with isotropic thermal parameters except for the bound water molecules in **4** which were not refined, and the carbon atoms in **4** which were refined anisotropically. The Re−O bond distances and site occupancies for the oxygen atoms of the bound water molecules in **4** were fixed at 2.13 Å and 25%, respectively. Heavy atoms ($Z > 9$) were refined anisotropically in all three structures. Crystallographic parameters are listed in Table 1.

High-resolution X-ray powder diffraction data were collected for compounds **6** and **7** at beamline 2-1 of the Stanford Synchrotron Radiation Laboratory. Finely ground powders of the hydrated samples were loaded into 0.5 mm glass capillaries under aerobic conditions. X-rays of wavelength 1.27727(1) or 1.28077(1) Å were selected using a Si(111) monochromator. Data for compound **6** were collected in *Q*-space ($Q = 2\pi/d$) over the range 0.4269−7.4978 Å^{-1} ($2\theta = 5-96°$) with 0.003 Å^{-1} steps, while data for compound **7** were collected in 2θ mode over the range 5−120° with 0.05° steps. The wavelength, zero point, and profile parameters were refined using a Si standard (NIST 640b). The crystal structure of **4** with adjusted site occupancies was adopted as a starting model for Rietveld refinements against the diffraction data using the program GSAS.[17] A cosine Fourier series background, diffuse scattering parameters,[18] and a pseudo-Voigt peak shape[19]

(17) Larson, A. C.; von Dreele, R. B. *GSAS: General Structure Analysis System*; Los Alamos National Laboratory: Los Alamos, NM, 1990.

(18) Lawson, A. C.; Martinez, B.; von Dreele, R. B.; Roberts, J. A.; Sheldon, R. I.; Bruin, T. O. *Philos. Mag. B* **2000**, *80*, 1869.

(19) Thompson, P.; Cox, D. E.; Hastings, J. B. *J. Appl. Crystallogr.* **1987**, *20*, 79.

(corrected[20] for asymmetry) were all also refined. Locations of the oxygen atoms in solvate water molecules were determined using difference Fourier maps. The molecular geometry of the $[Re_6Se_8(CN)_6]^{3-}$ cluster (as established in the structure of **2**·$3H_2O$) was maintained by imposing the following restraints: Re−Re 2.6(1) Å, Re−Se 2.52(1) Å, Re−C 2.13(5) Å, and C−N 1.15(5) Å. Anisotropic thermal parameters were refined for the Re and Se atoms, and isotropic thermal parameters were refined for the Ni and Ga atoms. The thermal parameters for C, N, and metal-bound O atoms were fixed at an isotropic value of 0.025 $Å^2$; thermal parameters for O atoms in solvate water molecules were fixed at 0.06 $Å^2$. Crystallographic parameters for both structures are listed in Table 1.

Gas Sorption Measurements. Samples[21] were evacuated for at least 12 h on a vacuum manifold to a pressure of no more than 5 mTorr. Sample tubes were oven dried, sealed under dinitrogen using a seal frit, and weighed precisely. Samples were quickly transferred into the sample tube under aerobic conditions. Degassing proceeded on a Micromeritics ASAP 2010 analyzer with heating at 75 °C and evacuation to a pressure of at most 15 μTorr. The degassed sample and sample tube were weighed precisely (with the seal frit preventing exposure of the sample to air after degassing) and then transferred back to the analyzer. Measurements were performed at 77 K in a liquid nitrogen bath. Once each measurement was complete, the structural integrity of the sample was confirmed by X-ray powder diffraction.

Other Physical Measurements. Routine X-ray powder diffraction data were collected using Cu Kα ($\lambda = 1.5406$ Å) radiation on a Siemens D5000 diffractometer. Infrared spectra were recorded on a Nicolet Avatar 360 FTIR spectrometer equipped with a horizontal attenuated total reflectance accessory. Cyclic voltammetry was performed using a Bioanalytical systems CV-50W voltammagraph, a 0.1 M solution of Bu_4NBF_4 in methanol as the supporting electrolyte, and a platinum working electrode. Potentials were determined vs a $Ag/AgNO_3$ reference electrode. Thermogravimetric analyses were carried out at a ramp rate of 1 °C/min under a dinitrogen atmosphere, using a TA Instruments TGA 2950. Magnetic susceptibility data were measured on a Quantum Design MPMS2 SQUID Magnetometer. Field emission scanning electron microscopy (SEM) and transmission electron microscopy (TEM) images were obtained using JEOL 6340 and JEOL 002B electron microscopes, respectively.

Results and Discussion

Syntheses. In a fortuitous parallel with $[Fe(CN)_6]^{4-}$, the $[Re_6Se_8(CN)_6]^{4-}$ cluster readily undergoes a one-electron oxidation to give an isolable trianion. As measured by cyclic voltammetry, the $[Re_6Se_8(CN)_6]^{3-/4-}$ couple occurs at $E_{1/2} =$ 0.66, 0.37, and 0.32 V vs SCE in water,[5e] methanol, and acetonitrile,[22] respectively. Accordingly, treatment of an orange solution of $(Bu_4N)_4[Re_6Se_8(CN)_6]$ (**1**) in methanol with iodine affords the oxidized green compound $(Bu_4N)_3[Re_6Se_8(CN)_6]$ (**2**). Subsequent metathesis with sodium perchlorate in acetonitrile then provides the water-soluble salt $Na_3[Re_6Se_8(CN)_6]$ (**3**). Like $[Fe(CN)_6]^{3-}$,[10] the oxidized cluster is unstable in aqueous solution, gradually reducing back to the tetraanion over the course of several days—presumably according to the following reaction.

$$4[Re_6Se_8(CN)_6]^{3-} + 2H_2O \rightarrow 4[Re_6Se_8(CN)_6]^{4-} + 4H^+ + O_2 \quad (4)$$

The oxidized cluster is, however, stable in organic solvents such as methanol and acetonitrile for extended periods of time. In certain other solvents, spontaneous oxidation of $[Re_6Se_8(CN)_6]^{4-}$ by dioxygen appears to occur: red-green dichroic crystals of **2**·$3H_2O$ were obtained from a 1,2-propanediol solution of **1** upon cooling from 80 °C to room temperature under aerobic conditions. The infrared spectrum of compound **2** exhibits a strong, sharp absorption band at $\nu_{CN} = 2123$ cm^{-1}, which, consistent with the increased charge of the cluster core,[23] is 17 cm^{-1} higher in energy than the corresponding band in the spectrum of compound **1**.

The reaction between $[Fe(H_2O)_6]^{3+}$ and $[Re_6Te_8(CN)_6]^{4-}$ in aqueous solution closely follows the synthesis of Prussian blue (reaction 1), immediately precipitating the expanded analogue $Fe_4[Re_6Te_8(CN)_6]_3$·$27H_2O$.[5b] With $[Re_6Se_8(CN)_6]^{4-}$, however, the corresponding reaction is rather more complicated. At room temperature, it produces a crystalline black solid of undetermined composition, exhibiting an X-ray powder diffraction pattern that indexes to a primitive tetragonal unit cell with $a =$ 19.17 Å and $c = 22.89$ Å. While standing under the mother liquor for two months, this solid slowly dissolves to reemerge as black square prism-shaped crystals of $Fe_4[Re_6Se_8(CN)_6]_3$·$36H_2O$ (**4**). The process is accelerated at elevated temperatures, and simply heating the initial reaction mixture at 75 °C for several hours is sufficient to produce a microcrystalline form of compound **4**:

$$4[Fe(H_2O)_6]^{3+} + 3[Re_6Se_8(CN)_6]^{4-} \xrightarrow{\Delta} Fe_4[Re_6Se_8(CN)_6]_3\cdot 36H_2O \quad (5)$$

Under such conditions, the rate of hydrolysis of $[Fe(H_2O)_6]^{3+}$ also increases, making it necessary to acidify the reaction solutions to prevent the coprecipitation of amorphous iron hydroxide phases. Similar variations of reaction temperature and pH have been used to control purity, particle size, and crystallinity in the preparation of Prussian blue.[24] If reaction 5 is carried out at too low of a pH (below ca. 3), the product is contaminated with a second phase, $H[cis\text{-}Fe(H_2O)_2][Re_6Se_8(CN)_6]$·$2H_2O$ (**8**). This compound is readily prepared in pure form from highly acidic reactions performed at a slightly lower temperature. As with $Fe_4[Re_6Te_8(CN)_6]_3$·$27H_2O$,[5b] the black color of compounds **4** and **8** is attributed to a cluster-to-metal charge-transfer band analogous to the metal-to-metal charge-transfer band responsible for the color of Prussian blue.[25]

Similarly, the reactivity of the $[Re_6Se_8(CN)_6]^{3-}$ cluster approximates that of a trianionic hexacyanometalate complex such as $[Fe(CN)_6]^{3-}$. For example, the reaction between nickel(II) perchlorate and $Na_3[Re_6Se_8(CN)_6]$ (**3**) in aqueous solution yields $Ni_3[Re_6Se_8(CN)_6]_2$·$33H_2O$ (**6**), in direct analogy with the preparation of $Ni_3[Fe(CN)_6]_2$·$14H_2O$[14b,d] (see reaction 3, above):

$$3[Ni(H_2O)_6]^{2+} + 2[Re_6Se_8(CN)_6]^{3-} \xrightarrow{\Delta} Ni_3[Re_6Se_8(CN)_6]_2\cdot 33H_2O \quad (6)$$

Here again, heat is required to obtain a crystalline cubic framework. At room temperature, reaction 6 immediately precipitates an amorphous green solid, characterized by an essentially featureless X-ray powder diffraction pattern. However, as shown in Figure 2, when the reaction mixture is subsequently heated at 60 °C, the crystallinity of the solid

(20) Finger, L. W.; Cox, D. E.; Jephcoat, A. P. *J. Appl. Crystallogr.* **1994**, *27*, 892.

(21) Compound **6** was soaked in acetone for approximately 5 h prior to evacuation. In addition, after evacuation and loading into the sample tube, one drop of acetone was added directly to this sample before it was degassed. All other samples were used as prepared.

(22) Yoshimura, T.; Ishizaka, S.; Sasaki, Y.; Kim, H. B.; Kitamura, N.; Naumov, N. G.; Sokolov, M. N.; Fedorov, V. E. *Chem. Lett.* **1999**, *10*, 1121.

(23) Jones, L. H. *Inorg. Chem.* **1963**, *2*, 777.

(24) Wilde, R. E.; Ghosh, S. N.; Marshall, B. J. *Inorg. Chem.* **1970**, *9*, 2512.

(25) Robin, M. B. *Inorg. Chem.* **1962**, *1*, 337.

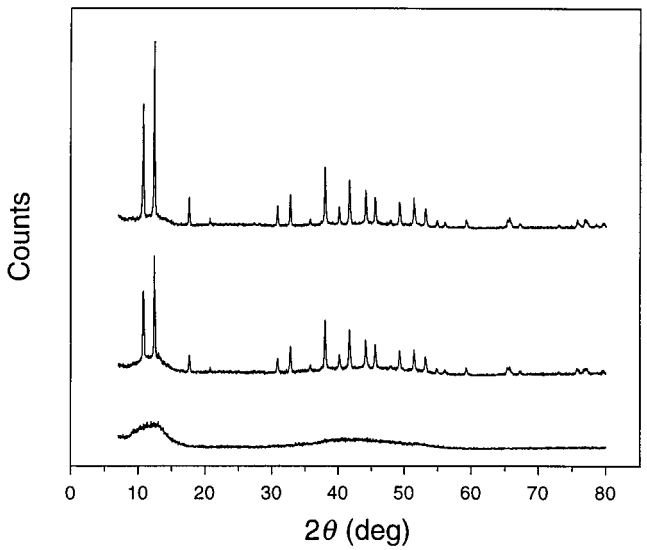

Figure 2. Powder X-ray diffraction data for compound **6**, as prepared by heating the solid in water at 60 °C for 0 (lower), 2 (middle), and 12 h (upper).

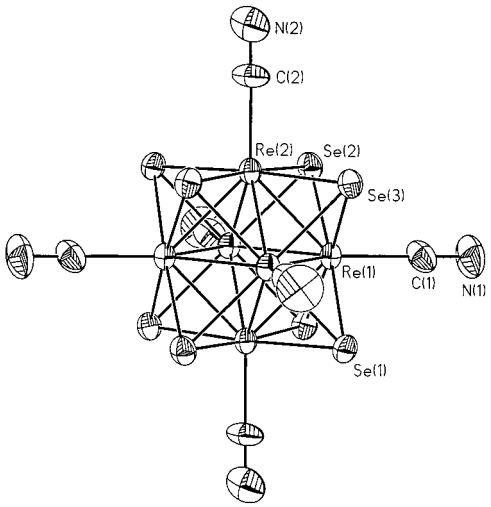

Figure 3. The $[Re_6Se_8(CN)_6]^{3-}$ cluster, as observed in the structure of **2**·$3H_2O$. Ellipsoids are drawn at the 40% probability level. The cluster resides on a 2/*m* symmetry site, with atoms Re(2), Se(1), Se(3), C(2), and N(2) situated in the mirror plane

gradually increases, until, after 12 h, no further change is evident in the resulting face-centered cubic diffraction pattern. This period of heating affords sizable crystallites with a truncated cube morphology and edge dimensions in the range 1−3 μm (as probed by SEM). An excess of $[Ni(H_2O)_6]^{2+}$ is also employed in reaction 6 to prevent contamination of the product with H[*cis*-$Ni(H_2O)_2$][$Re_6Se_8(CN)_6$]·$2H_2O$ (**10**). By replacing $[Ni(H_2O)_6]^{2+}$ with $[Co(H_2O)_6]^{2+}$, the synthesis of $Co_3[Re_6Se_8(CN)_6]_2$·$25H_2O$ (**5**) is accomplished in much the same fashion, albeit with one important difference. Heating the reaction mixture is limited to a period of just 20 min, since more extended heating leads to reduction of the cluster and, ultimately, formation of $[Co(H_2O)_3]_4[Co_2(H_2O)_4][Re_6Se_8(CN)_6]_3$·$44H_2O$.[5d] In contrast, compound **6** can be heated in its mother liquor at 100 °C for several weeks without degrading. The more limited heating period utilized in preparing compound **5** yields aggregates of much smaller cube-shaped nanocrystals with edge-dimensions in the range 30−60 nm (as probed by TEM). Attempts at using acid to inhibit reduction of the cluster in the preparation of **5** led to isolation of H[*cis*-$Co(H_2O)_2$][$Re_6Se_8(CN)_6$]·$2H_2O$ (**9**).

The $[Re_6Se_8(CN)_6]^{3-}$ cluster also mimics $[Fe(CN)_6]^{3-}$ in its reactions with metal trications. Emulating the synthesis of Ga[$Fe(CN)_6$]·xH_2O,[10d] $Na_3[Re_6Se_8(CN)_6]$ (**3**) reacts with gallium nitrate in aqueous solution to give Ga[$Re_6Se_8(CN)_6$]·$6H_2O$ (**7**):

$$[Ga(H_2O)_6]^{3+} + [Re_6Se_8(CN)_6]^{3-} \xrightarrow{\Delta} Ga[Re_6Se_8(CN)_6]\cdot 6H_2O \quad (7)$$

As with reaction 5 above, this reaction produces an intermediate phase of unknown composition at room temperature. X-ray analysis of a green single crystal revealed a primitive tetragonal unit cell with $a = 19.164(2)$ Å and $c = 22.903(3)$ Å, similar to that observed for the iron-containing intermediate; unfortunately, the crystal was too small to permit a complete structure determination. By carrying out reaction 7 in an acidic solution at 80 °C for 30 min, however, green compound **7** is readily prepared in pure form. As with compound **5**, the limited heating time yields aggregates of nanocrystals. Note that heating the reaction more extensively yields a partially reduced yellow-green product exhibiting a lower μ_{eff} and a slightly higher water content, indicating the presence of a small amount of $Ga_4[Re_6Se_8(CN)_6]_3$·$38H_2O$.

Consistent with the foregoing trends in thermal stability, after two months of storage in air, the green compounds $Co_3[Re_6Se_8(CN)_6]_2$·$25H_2O$ (**5**) and Ga[$Re_6Se_8(CN)_6$]·$6H_2O$ (**7**) degrade into less-crystalline orange-brown solids, while $Ni_3[Re_6Se_8(CN)_6]_2$·$33H_2O$ (**6**) shows no signs of decomposition. These differences in stability likely arise from variations in the electron-withdrawing ability of the metal ions coordinated to the $[Re_6Se_8(CN)_6]^{3-}$ cluster. Electrochemical measurements show that the $[Fe(CN)_6]^{3-}$ units in Prussian blue analogues are more easily reduced as the ionic potential (the charge divided by the effective radius) of the coordinated metal ions increases.[26] This trend is accompanied by a decrease in σ-donation of the cyanide ligand to the iron center, as deduced from an increase in the cyanide stretching frequency in the infrared spectrum.[27] Analogously, the $[Re_6Se_8(CN)_6]^{3-}$ clusters in expanded Prussian blue type solids should be more easily reduced as the ionic potential of the coordinated metal ions increases. Thus, the greater electron-withdrawing ability of Ga^{3+} ions versus Ni^{2+} ions leads to compound **7** being less stable toward reduction by water than compound **6**. In the case of compound **5**, decomposition appears to involve oxidation of some of the Co^{2+} ions to Co^{3+} ions (signaled by the appearance of a new band in the infrared spectrum at $\nu_{CN} = 2200$ cm^{-1}),[28] which then facilitates reduction of the clusters by water.

Structures. Figure 3 displays the structure of the oxidized $[Re_6Se_8(CN)_6]^{3-}$ cluster, as present in $(Bu_4N)_3[Re_6Se_8(CN)_6]$·$3H_2O$ (**2**·$3H_2O$). Overall, the cluster maintains the familiar face-capped octahedral motif[29] of the tetraanion, consisting of a central Re_6 octahedron with each face capped by a μ_3-Se atom and each vertex bound by a radially projecting cyanide ligand. Its metric parameters (see Table 2) are nearly identical to those

(26) Scholz, F.; Dostal, A. *Angew. Chem., Int. Ed. Engl.* **1995**, *34*, 2685.

(27) Bertrán, J. F.; Pascual, J. B.; Ruiz, E. R. *Spectrochim. Acta, Part A* **1990**, *46*, 685.

(28) Interestingly, the cyanide stretching frequencies in the infrared spectra of Prussian blue analogues incorporating $[Re_6Se_8(CN)_6]^{3-}$ clusters are nearly identical to those observed in the corresponding compounds containing $[Fe(CN)_6]^{3-}$,[26] differing by no more than a few wavenumbers.

(29) This geometry is common to a wide variety of transition metal halide and chalcogenide clusters: (a) Lee, S. C.; Holm, R. H. *Angew. Chem., Int. Ed. Engl.* **1990**, *29*, 840 and references therein. (b) Goddard, C. A.; Long, J. R.; Holm, R. H. *Inorg. Chem.* **1996**, *35*, 4347 and references therein.

Table 2. Selected Mean Interatomic Distances (Å) and Angles (deg) from the Structures of $(Bu_4N)_3[Re_6Se_8(CN)_6]\cdot 3H_2O$ (**2**·$3H_2O$), $Fe_4[Re_6Se_8(CN)_6]_3\cdot 36H_2O$ (**4**), $Ni_3[Re_6Se_8(CN)_6]_2\cdot 33H_2O$, (**6**), $Ga[Re_6Se_8(CN)_6]\cdot 6H_2O$ (**7**), and $H[cis\text{-}Fe(H_2O)_2][Re_6Se_8(CN)_6]\cdot 2H_2O$ (**8**).

	2·$3H_2O$	**4**	**6**	**7**	**8**
Re−Re	2.632(5)	2.6322(1)	2.637(3)	2.627(3)	2.639(7)
Re−Se	2.519(8)	2.523(2)	2.515(2)	2.505(1)	2.522(6)
Re−C	2.06(1)	2.11(2)	2.05(1)	2.138(8)	2.09(3)
C−N	1.115(7)	1.11(3)	1.105(2)	1.170(8)	1.18(5)
M−N		2.05(3)	2.10(2)	1.89(1)	2.06(3)
M−O		2.13(2)	2.02		2.11
Se−Re−C	91.8(7)	91.77(4)	91.99(6)	91.99(6)	92(3)
Re−C−N	178	180	180	180	174(3), 180
M−N−C		180	180	180	152(2), 175(2)
N−M−N		90	90	90	94(3)
O−M−O		90	90		87.0(7)
N−M−O		90	90		88(2)

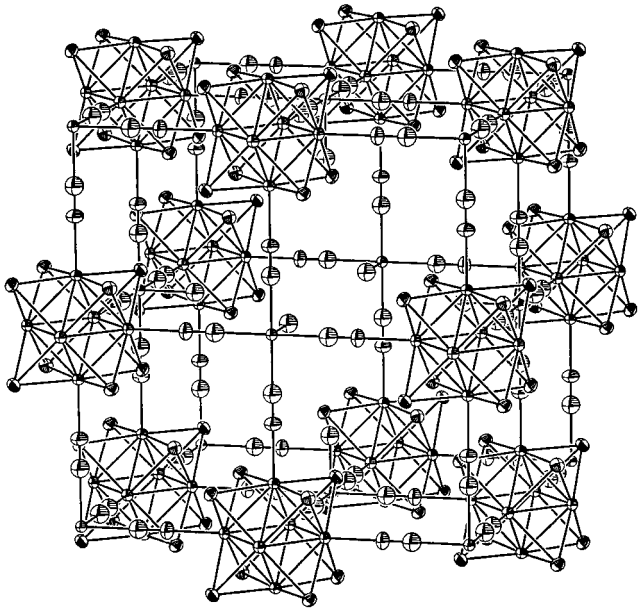

Figure 4. Cubic unit cell from the structure of $Fe_4[Re_6Se_8(CN)_6]_3\cdot 36H_2O$ (**4**). Ellipsoids are drawn at the 40% probability level; solvate water molecules and hydrogen atoms have been omitted for clarity. Atom types are analogous to those in Figure 1 (right), with the exception of the ellipsoids displayed with only one bond, which represent oxygen atoms. A localized vacancy of the central $[Re_6Se_8(CN)_6]^{4-}$ cluster is depicted to reveal the average cavity geometry in the structure (see Figure 1 for comparison). Note how water molecules coordinate the exposed Fe^{3+} ion sites.

observed for the $[Re_6Se_8(CN)_6]^{4-}$ cluster:[5a] the only noteworthy difference is a slight decrease in the Re−C bond distances from a mean of 2.10(2) Å to a mean of 2.06(1) Å upon oxidation, consistent with the increased charge of the cluster core. Bearing the same charge and an equivalent arrangement of the cyanide ligands, the $[Re_6Se_8(CN)_6]^{3-}$ cluster represents an enlarged analogue of $[Fe(CN)_6]^{3-}$, wherein the mean *trans*-N···N distance has increased from 6.17(1) Å[30] to 10.08(4) Å.

Replacement of the $[Fe(CN)_6]^{4-}$ units in a cubic Prussian blue type structure by $[Re_6Se_8(CN)_6]^{4-}$ clusters (see Figure 1) was previously demonstrated with the synthesis of $Ga_4[Re_6Se_8(CN)_6]_3\cdot 38H_2O$.[5b] Sizable crystals of the cluster-containing phase could not be obtained, however, such that its structure determination had to rely upon the interpretation and profile analysis of powder X-ray diffraction data. Similar difficulties plagued

(30) Figgis, B. N.; Skelton, B. W.; White, A. H. *Aust. J. Chem.* **1978**, *31*, 1195.

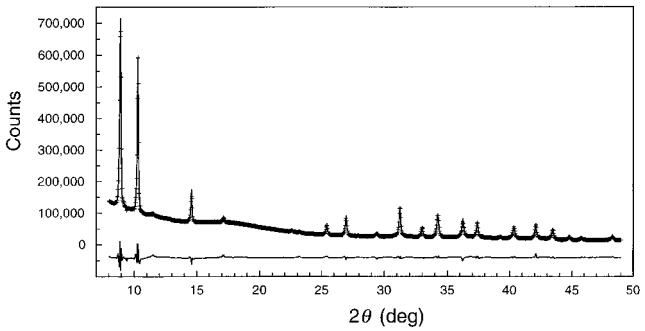

Figure 5. A portion of the powder X-ray diffraction data for compound **6** (crosses) along with the final fit from the crystallographic analysis (upper solid line). The lower solid line plots the difference between the observed and simulated patterns.

the study of Prussian blue, and it was not until 1972 that crystals suitable for a single-crystal X-ray analysis were finally produced.[8] Fortunately, the growth of high-quality single crystals of the new compound $Fe_4[Re_6Se_8(CN)_6]_3\cdot 36H_2O$ (**4**) via the gradual redissolution technique described above permitted a full crystallographic refinement of its structure. The results show compound **4** to be isostructural with $Ga_4[Re_6Se_8(CN)_6]_3\cdot 38H_2O$, possessing a three-dimensional cubic framework that represents a direct expansion of the Prussian blue structure. Analogous to the situation in Prussian blue, charge balance leads to an occupancy of only 75% for the $[Re_6Se_8(CN)_6]^{4-}$ cluster sites, creating large water-filled cavities in the framework. These cavities have an average structure defined by the cubic cage obtained upon removing the central $[Re_6Se_8(CN)_6]^{4-}$ cluster from the unit cell, as depicted in Figure 4. Each such cage contains a total of 36 water molecules, six of which coordinate the exposed Fe^{3+} ions centering the cube faces. In contrast to the crystals of Prussian blue that were analyzed,[8] crystals of **4** display no evidence for a primitive cubic unit cell owing to partial ordering of the lattice vacancies. Mean interatomic distances and angles from the structure are listed in Table 2; the Fe−N and Fe−O distances are approximately the same as those reported for Prussian blue (2.05(3) and 2.13(2) Å, respectively).[8]

The structures of the closely related phases $Ni_3[Re_6Se_8(CN)_6]_2\cdot 33H_2O$ (**6**) and $Ga[Re_6Se_8(CN)_6]\cdot 6H_2O$ (**7**) were established with Rietveld refinements against synchrotron X-ray powder diffraction data. In both cases, the crystal structure of compound **4** was adapted for use as an initial structural model. The fit to the low-angle portion of the data resulting from refinement of the former structure is shown in Figure 5; fits to the entire range of data from both refinements have been deposited as Supporting Information. The structure of compound **7** consists of a fully occupied cubic lattice of alternating Ga^{3+} ions and $[Re_6Se_8(CN)_6]^{3-}$ clusters, as depicted at the right in Figure 1. With no cluster vacancies, the cavities in the three-dimensional framework are defined by the cubelike $Ga_4(Re_6Se_8)_4(CN)_{12}$ cages comprising a single octant of the unit cell; each such cage encapsulates three water molecules. The structure of compound **6** is based on the same type of three-dimensional framework, but with one-third of the $[Re_6Se_8(CN)_6]^{3-}$ clusters missing from the lattice owing to the reduced charge of the Ni^{2+} ions. Thus, of the four total cluster positions per face-centered cubic unit cell, one and one-third are actually vacant, giving rise to larger framework cavities than found in either compounds **4** or **7**. On average, for each missing cluster *at least* one of the twelve surrounding cluster sites (see Figure 4) is also vacant, resulting in a framework in which the smallest cavities are typically defined by the cage depicted in Figure 6.

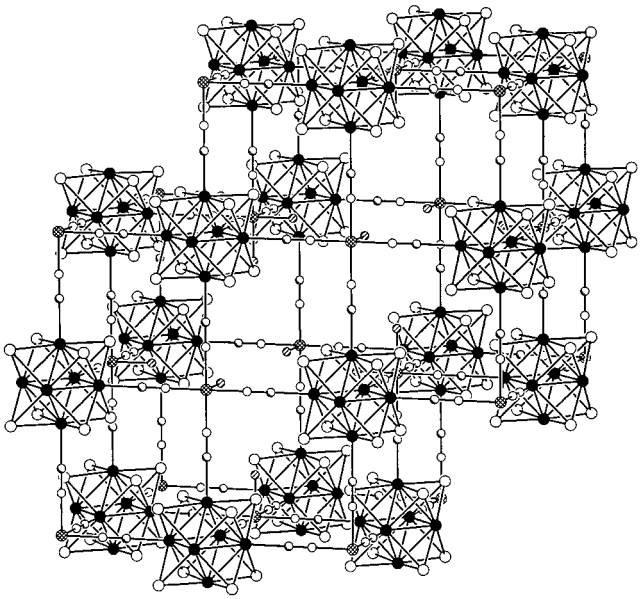

Figure 6. Cage defining the smallest cavities in the structure of $Ni_3[Re_6Se_8(CN)_6]_2 \cdot 34H_2O$ (**6**). Black, large white, crosshatched, shaded, small white, and hatched spheres represent Re, Se, Ni, C, N, and O atoms, respectively; solvate water molecules and hydrogen atoms have been omitted for clarity. Note how water molecules coordinate the exposed Ni^{2+} ion sites.

Indeed, in two out of three instances, two of the surrounding cluster sites will be vacant, leading to even larger cavities. Note that the structures of compounds **6** and **7** represent direct expansions of the Prussian blue analogues $Ni_3[Fe(CN)_6]_2 \cdot 14H_2O$[14b,d] and $Ga[Fe(CN)_6] \cdot xH_2O$, respectively;[10d] mean interatomic distances and angles from both structures are compared in Table 2. X-ray powder diffraction data indicate that $Co_3[Re_6Se_8(CN)_6]_2 \cdot 25H_2O$ (**5**) is isostructural to compound **6**.

The crystal structure of $H[cis\text{-}Fe(H_2O)_2][Re_6Se_8(CN)_6] \cdot 2H_2O$ (**8**) reveals a more densely packed three-dimensional framework in which $[Re_6Se_8(CN)_6]^{4-}$ clusters are linked through a combination of $[cis\text{-}Fe(H_2O)_2]^{3+}$ units and protons (see Figure 7). Each hexacyanide cluster is surrounded by four Fe^{3+} ions and two protons arranged in a *trans* configuration. The protons serve to connect the clusters into linear one-dimensional chains extending along the 2-fold rotation axes and perpendicular to the 3_1 screw axes in the structure. The short N···N separation of 2.50(3) Å reflects the strength of the hydrogen bonding in the N−H···N bridges (which are presumably still slightly asymmetric).[31,32] This represents one of the closest contacts observed for a hydrogen-bonding interaction; to our knowledge, the shortest N···N distance reported previously is 2.526(3) Å for the protonated "proton sponge" 1,6-diazabicyclo[4.4.4]-tetradecane hydrochloride.[32] Analogous bridging interactions with minimum N···N distances falling in the range 2.582−2.68 Å have been documented in the crystal structures of $H_4[Fe(CN)_6]$, $H_3[Fe(CN)_6]$, and $H_3[Co(CN)_6]$.[33] The chains of proton-bridged clusters in the structure of **8** are interconnected through iron(III) centers possessing an octahedral coordination environment with four cyanide ligands and two terminal water ligands. As evident in Figure 7, the Re−C−N−Fe bridges running parallel to the 3_1 screw axis are significantly bent, with mean Re−C−N and C−N−Fe angles of 174(3)° and 152(2)°, respectively. Other interatomic distances and angles from the structure are listed in Table 2. The close packing of the cluster units leaves little open space within the framework, such that the largest pores encapsulate a single solvate water molecule, which is located within hydrogen-bonding distance (O···O 2.665 Å) of a coordinated water molecule. X-ray powder diffraction data show the green compounds $H[cis\text{-}Co(H_2O)_2][Re_6Se_8(CN)_6] \cdot 2H_2O$ (**9**) and $H[cis\text{-}Ni(H_2O)_2][Re_6Se_8(CN)_6] \cdot 2H_2O$ (**10**) to be

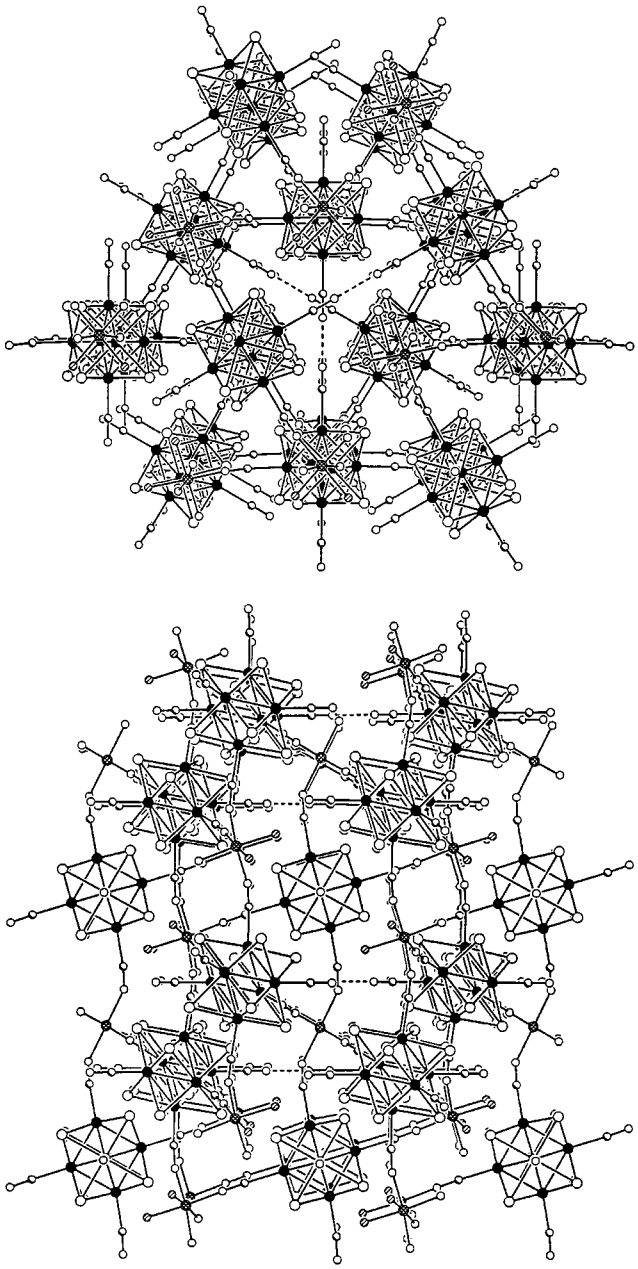

Figure 7. Views along (top) and perpendicular to (bottom) the 3_1 screw axis in the crystal structure of $H[cis\text{-}Fe(H_2O)_2][Re_6Se_8(CN)_6] \cdot 2H_2O$ (**8**). Large black, white, and crosshatched spheres represent Re, Se, and Fe atoms, respectively, while smaller highlighted, white, and diagonally shaded spheres represent C, N, and O atoms, respectively. Dashed lines indicate N−H···N interactions, which coincide with crystallographic 2-fold rotation axes; indeed, all clusters and Fe atoms reside along 2-fold rotation axes.

(31) Note that the hydrogen atoms were not located in the crystal structure.

(32) (a) Alder, R. W.; Orpen, A. G.; Sessions, R. B. *J. Chem. Soc., Chem. Commun.* **1983**, 999. (b) Malarski, Z.; Sobczyk, L.; Grech, L. *J. Mol. Struct.* **1988**, *177*, 339.

(33) (a) Pierrot, M.; Kern, R.; Weiss, R. *Acta Crystallogr.* **1966**, *20*, 425. (b) Güdel, H. U.; Ludi, A.; Fischer, P.; Halg, W. *J. Chem. Phys.* **1970**, *53*, 1917. (c) Haser, P. R.; de Broin, C. E.; Pierrot, M. *Acta Crystallogr.* **1972**, *B28*, 2530.

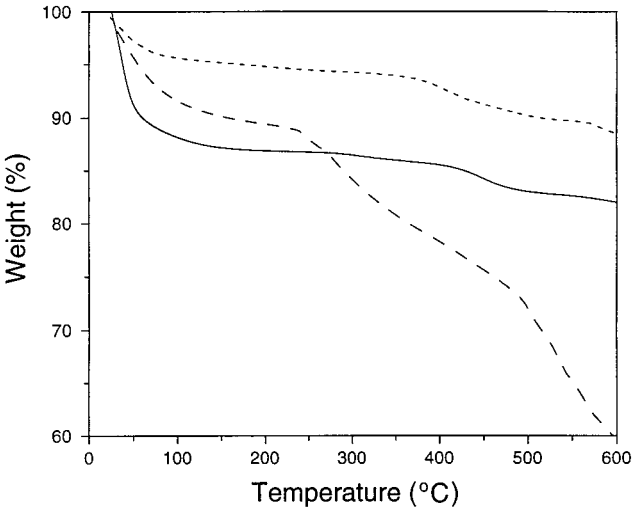

Figure 8. Thermogravimetric analyses showing weight loss in compounds **4** (longer dashes), **6** (solid line), and **7** (shorter dashes) with temperature increasing at a rate of 1 deg C/min.

isostructural to compound **8**, with Co^{2+} or Ni^{2+} ions substituting for the Fe^{3+} ions and $[Re_6Se_8(CN)_6]^{3-}$ substituting for $[Re_6Se_8(CN)_6]^{4-}$.

Thermal Stability. Thermogravimetric analyses were performed to probe the thermal stability of each new solid phase. Figure 8 shows the weight losses for the expanded Prussian blue analogues $Fe_4[Re_6Se_8(CN)_6]_3 \cdot 36H_2O$ (**4**), $Ni_3[Re_6Se_8(CN)_6]_2 \cdot 33H_2O$ (**6**), and $Ga[Re_6Se_8(CN)_6] \cdot 6H_2O$ (**7**) with increasing temperature. Analysis of $Co_3[Re_6Se_8(CN)_6]_2 \cdot 25H_2O$ (**5**) produced results similar to those obtained for compound **6**. All of the compounds dehydrate completely by ca. 150 °C, at which point the differences in percent weight lost reflect the expected variations in framework porosity due to the cluster vacancies. Compound **4** then begins to lose mass again as the temperature rises above 250 °C. A comparable trend is observed for Prussian blue, and has been attributed to the gradual evolution of cyanogen from the surfaces of the crystallites.[34] In contrast, compounds **5**−**7** can be heated to ca. 400 °C before displaying any further significant weight loss. The less robust nature of iron-containing metal−cyanide frameworks has been noted previously in comparing thermogravimetric analyses of $Fe_4[Re_6Te_8(CN)_6]_3 \cdot 27H_2O$ and $Ga_4[Re_6Se_8(CN)_6]_3 \cdot 38H_2O$.[5b] This characteristic also extends to the compounds $H[cis\text{-}M(H_2O)_2][Re_6Se_8(CN)_6] \cdot 2H_2O$ (M = Fe (**8**), Co (**9**), Ni (**10**)), which exhibit thermal profiles analogous to those of **4**, **5**, and **6**, respectively, albeit with a much smaller decrease in weight upon dehydration.

Dehydrating compounds **4**−**10** does not induce a loss of framework structure. Powder samples were heated at 250 °C for 6 h under a flow of dinitrogen, and were then characterized by X-ray diffraction. In each case, the results indicate preservation of the original crystal structure; however, the diffraction patterns for the expanded Prussian blue analogues **4**−**7** exhibit line shifts signifying a minor contraction of the cubic unit cell. A least-squares analysis of the data for compound **6** revealed a reduction of the cell parameter *a* from 14.2364(2) to 14.024(6) Å upon dehydration, corresponding to a 4.4% reduction in unit cell volume. A slightly smaller reduction in volume of 2.6% occurs with loss of water from $Ga_4[Re_6Se_8(CN)_6]_3 \cdot 38H_2O$. This effect has also been observed in Prussian blue, for which neutron powder diffraction studies revealed the contracted unit cell of the dehydrated solid to be associated with a slight buckling of the cyanide bridges away from linearity.[35]

(34) Seifer, G. B. *Russ. J. Inorg. Chem.* **1960**, *5*, 33.

Table 3. Water Content, Void Volume, and Percent Void Space Per Unit Cell for Representative Prussian Blue Analogues[a]

	no. water	void volume (Å^3)[b]	% void[b]
$Fe[Fe(CN)_6] \cdot 2H_2O$	8	480	44
$Fe_4[Fe(CN)_6]_3 \cdot 14H_2O$	14	557	53
$Ni_3[Fe(CN)_6]_2 \cdot 14H_2O$	19	640	58
$Ga[Re_6Se_8(CN)_6] \cdot 6H_2O$	24	1174	42
$Ga_4[Re_6Se_8(CN)_6]_3 \cdot 38H_2O$	38	1579	56
$Ni_3[Re_6Se_8(CN)_6]_2 \cdot 33H_2O$	44	1732	61

[a] All entries are per face-centered cubic unit cell (see Figure 1). [b] Upon dehydration, and neglecting any subsequent decrease in unit cell volume.[37]

Framework Porosity. The vacancies arising from charge balance create sizable cavities in the metal−cyanide framework of a Prussian blue analogue. Consequently, framework porosity increases as the cyanometalate site occupancy factors decrease from 1.00 to 0.75 to 0.67 along the series of representative compounds $Fe[Fe(CN)_6] \cdot 2H_2O$, $Fe_4[Fe(CN)_6]_3 \cdot 14H_2O$, and $Ni_3[Fe(CN)_6]_2 \cdot 14H_2O$.[36] As synthesized, water molecules fill the nonframework volume in the structures of these solids, such that the number of water molecules per face-centered cubic unit cell (see Figure 1, left) is a manifestation of the framework porosity. Table 3 shows how the water content correlates with the void volume[37] created within the structure upon dehydration. Gas sorption measurements provide perhaps the best experimental means of probing the accessibility of this void space. Figure 9 displays the dinitrogen sorption isotherm obtained for a dehydrated sample of Prussian blue. The solid continues to adsorb dinitrogen until the molecules fill the internal micropores and cover the external surfaces, resulting in an initial sharp rise in sorption followed by a plateau. Thus, dehydrated Prussian blue exhibits a Type I sorption isotherm characteristic of microporous solids.[38] To our knowledge, gas sorption isotherms have not been reported previously for Prussian blue or any of its analogues.[39]

Similar variations in framework porosity are realized in the expanded Prussian blue analogues incorporating $[Re_6Se_8(CN)_6]^{3-/4-}$ clusters. As evident from a comparison of the structures of $Fe[Fe(CN)_6] \cdot 2H_2O$ and $Ga[Re_6Se_8(CN)_6] \cdot 6H_2O$, substituting the larger hexacyanide clusters for the hexacyanometalate units more than doubles the accessible volume within a unit cell (see Figure 1 and Table 3). Once again, the void volume increases with the frequency of framework vacancies along the series of representative compounds $Ga[Re_6Se_8(CN)_6] \cdot 6H_2O$ (**7**), $Ga_4[Re_6Se_8(CN)_6]_3 \cdot 38H_2O$, and $Ni_3[Re_6Se_8(CN)_6]_2 \cdot 33H_2O$ (**6**). The dinitrogen sorption isotherms obtained for dehydrated samples of these phases are shown in Figure 9, and confirm the trend of increasing framework porosity. Dehydrated compound **7** exhibits a Type II isotherm, where the dramatic rise in sorption at higher dinitrogen pressures is likely associated

(35) Herren, F.; Fischer, P.; Ludi, A.; Hälg, W. *Inorg. Chem.* **1980**, *19*, 956.

(36) It should be noted that this trend in framework porosity does not necessarily extend to Prussian blue analogues of composition $M_2[M'(CN)_6]$. At least in the case of $Cu_2[Fe(CN)_6]$, the best structural model seems to indicate the presence of interstitial Cu^{2+} ions in a cubic $\{Cu_3[Fe(CN)_6]_2\}^{2-}$ framework: Ayrault, S.; Jimenez, B.; Garnier, E.; Fedoroff, M.; Jones, D. J.; Loos-Neskovic, C. *J. Solid State Chem.* **1998**, *141*, 475.

(37) Void volumes are based on the estimated van der Waals radii of the framework atoms, and were calculated from the crystal structures using a Monte Carlo integration procedure described previously.[5b] For comparison, the calculated void volumes per formula unit of zeolite A ($Na_{12}[Al_{12}Si_{12}O_{48}]$) and zeolite ZSM-5 ($H_2[Al_2Si_{94}O_{192}] \cdot 24H_2O$) are 557 (30%) and 2365 Å (44%), respectively.

(38) Roquerol, F.; Rouquerol J.; Sing, K. *Adsorption by Powders and Solids: Principles, Methodology, and Applications*; Academic Press: London, 1999.

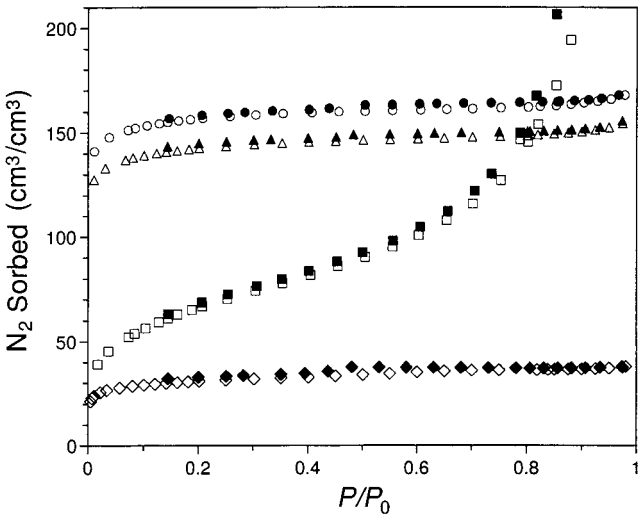

Figure 9. Dinitrogen sorption isotherms for $Fe_4[Fe(CN)_6]_3$ (diamonds), $Ga[Re_6Se_8(CN)_6]$ (squares), $Ga_4[Re_6Se_8(CN)_6]_3$ (triangles), and $Ni_3[Re_6Se_8(CN)_6]_2$ (circles) at 77 K. Adsorption and desorption are indicated by open and filled symbols, respectively. The ratio of gas pressure to saturation pressure, P/P_0, was obtained with $P_0 = 753$ Torr. Using the BET model, the surface areas of the foregoing compounds were determined to be 87.4, 229, 509, and 521 m^2/cm^3, respectively.[40]

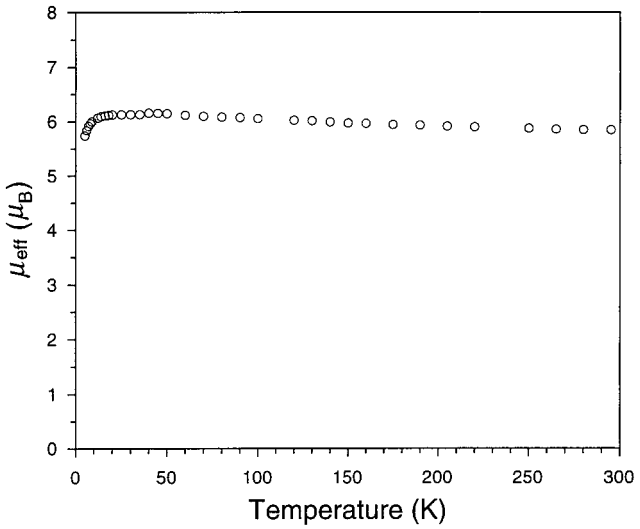

Figure 10. Magnetic behavior of compound **6**, as measured in an applied field of 1000 G.

with delayed capillary condensation within aggregates of nanocrystals.[38] The other solids consist of larger crystallites, and consequently maintain Type I isotherms. The substantially larger cavities in the cluster-containing phases lead to much higher sorption capacities than observed for Prussian blue. Although the percent void space is only slightly greater in $Ga_4[Re_6Se_8(CN)_6]_3$, its expanded cavities presumably permit a more efficient packing of the absorbed dinitrogen molecules than is possible in $Fe_4[Fe(CN)_6]_3$. The surface areas obtained from dinitrogen sorption data using the BET method are listed in the legend of Figure 9, and provide a further confirmation of the trend in framework porosity.

Magnetic Properties. The paramagnetic iron centers in $Fe_4[Re_6Se_8(CN)_6]_3 \cdot 36H_2O$ (**4**) and $H[cis\text{-}Fe(H_2O)_2][Re_6Se_8(CN)_6] \cdot 2H_2O$ (**8**) are well-separated by the intervening diamagnetic $[Re_6Se_8(CN)_6]^{4-}$ clusters. At room temperature, these compounds display effective magnetic moments of 12.11 and 6.03 μ_B, respectively, consistent with the presence of magnetically isolated high-spin Fe^{3+} ions. No evidence for magnetic ordering was observed in either phase at temperatures down to 5 K.

The oxidized cluster $[Re_6Se_8(CN)_6]^{3-}$ is paramagnetic, raising the possibility that it might engage in magnetic exchange coupling with the surrounding paramagnetic transition metal ions in expanded Prussian blue analogues.[12d,41] The effective magneticmoment of $(Bu_4N)_3[Re_6Se_8(CN)_6]$ (**2**) at room temperature is 2.08 μ_B, slightly higher than the spin-only value of 1.73 μ_B expected for one unpaired electron with $g = 2.00$. The higher moment is in line with the g value of 2.51 measured for $(Bu_4N)_3[Re_6Se_8I_6]$ in frozen DMF,[42] and with the effective moment of 2.05 μ_B established for the sulfur-containing cluster in $(Bu_4N)_3[Re_6S_8Cl_6]$.[43] Thus, $Ni_3[Re_6Se_8(CN)_6]_2 \cdot 33H_2O$ (**6**) contains a three-dimensional network in which $S = 1$ Ni^{2+} ions are linked to $S = {}^1/_2$ $[Re_6Se_8]^{3+}$ cluster cores through bridging cyanide ligands. The effective moment of this compound is plotted in Figure 10 for temperatures ranging from 5 to 295 K. Little deviation is observed from the room-temperature moment of 6.12 μ_B, indicating that no significant magnetic exchange coupling occurs between the spin centers. In distinct contrast, its noncluster analogue $Ni_3[Fe(CN)_6]_2 \cdot 14H_2O$ exhibits ferromagnetic coupling between the $S = 1$ Ni^{2+} ions and the $S = {}^1/_2$ Fe^{3+} ions, and behaves as a bulk ferromagnet at temperatures below 24 K.[44] The lack of coupling in compound **6** is most likely due to the nature of the orbital in which the unpaired spin of the cluster resides. Based on electronic structure calculations for face-capped octahedral clusters,[45] the unpaired electron is expected to be associated with a pair of e_g orbitals that are primarily Re−Re bonding in character. These orbitals have δ-type symmetry with respect to the cyanide ligands, and therefore do not interact with the σ- or π-type orbitals of the cyanide ligands utilized in magnetic superexchange.[46] Concor-

(39) Gas sorption isotherms have, however, been reported for dehydrated samples of $K_2Zn_3[Fe(CN)_6]_2 \cdot 9H_2O$, a compound featuring a noncubic framework with tetrahedral coordination of the Zn^{2+} ions. See: (a) Renaud, A.; Cartraud, P.; Gravereau, P.; Garnier, E. *Thermochim. Acta* **1979**, *31*, 243. (b) Cartraud, P.; Caintot, A.; Renaud, A. *J. Chem. Soc., Faraday Trans. 1* **1981**, *77*, 1561.

(40) Note that all values have been reported on a per volume basis to facilitate comparisons between frameworks having components with very different densities.

(41) Numerous noncluster Prussian blue analogues exhibit bulk magnetic ordering. (a) Gadet, V.; Mallah, T.; Castro, I.; Verdaguer, M. *J. Am. Chem. Soc.* **1992**, *114*, 9213. (b) Entley, W. R.; Girolami, G. S. *Science* **1995**, *268*, 397. (c) Ferlay, S.; Mallah, T.; Ouahès, R.; Veillet, P.; Verdaguer, M. *Nature* **1995**, *378*, 701. (d) Entley, W. R.; Treadway, C. R.; Girolami, G. S. *Mol. Cryst. Liq. Cryst.* **1995**, *273*, 153. (e) Dujardin, E.; Ferlay, S.; Phan, X.; Desplanches, C.; Cartier dit Moulin, C.; Sainctavit, P.; Baudelet, F.; Dartyge, E.; Veillet, P.; Verdaguer, M. *J. Am. Chem. Soc.* **1998**, *120*, 11347. (f) Holmes, S. M.; Girolami, G. S. *J. Am. Chem. Soc.* **1999**, *121*, 5593. (g) Hatlevik, Ø.; Buschmann, W. E.; Zhang, J.; Manson, J. L.; Miller, J. S. *Adv. Mater.* **1999**, *11*, 914. (h) Verdaguer, M.; Bleuzen, A.; Marvaus, V.; Vaissermann, J.; Seuleiman, M.; Desplanches, C.; Scuiller, A.; Train, C.; Garde, R.; Gelly, G.; Lomenech, C.; Rosenman, I.; Veillet, P.; Cartier, C.; Villain, F. *Coord. Chem. Rev.* **1999**, *190*, 1023 and references therein.

(42) Zheng, Z.; Gray, T. G.; Holm, R. H. *Inorg. Chem.* **1999**, *38*, 4888.

(43) Guilbaud, C.; Deluzet, A.; Domercq, B.; Molinié, P.; Coulon, C.; Boubekeur, K.; Batail, P. *Chem. Commun.* **1999**, 1867.

(44) Juszczyk, S.; Johansson, C.; Hanson, M.; Ratuszna, A.; Malecki, G. *J. Phys.: Condens. Matter* **1994**, *6*, 5697.

(45) (a) Hughbanks, T.; Hoffmann, R. *J. Am. Chem. Soc.* **1983**, *105*, 1150. (b) Hughbanks, T. *Prog. Solid State Chem.* **1989**, *19*, 329. (c) Lin, Z.; Williams, I. D. *Polyhedron* **1996**, *15*, 3277.

(46) Weihe, H.; Güdel, H. *Comments Inorg. Chem.* **2000**, *22*, 75.

(47) Rüegg, M.; Ludi, A.; Rieder, K. *Inorg. Chem.* **1971**, *10*, 1773.

(48) Garnier, E.; Gravereau, P.; Hardy, P. *Acta Crystallogr.* **1982**, *B38*, 1401.

(49) Mullica, D. F.; Sappenfield, E. L. *J. Solid State Chem.* **1989**, *82*, 168.

(50) Mullica, D. F.; Milligan, W. O.; Kouba, W. T. *J. Inorg. Nucl. Chem.* **1979**, *41*, 967.

(51) Schwartzen, M.; Babel, D. *Z. Anorg. Allg. Chem.* **2000**, *626*, 1921.

Table 4. Metal−Cyanide Framework Structure Types[a] and Examples of Their Cluster-Expanded Analogues

metal−cyanide framework	dim.	ref	cluster-expanded analogue	ref
$Ga[Fe(CN)_6]\cdot xH_2O$	3-D	10d	$Ga[Re_6Se_8(CN)_6]\cdot 6H_2O$ (**7**)	
$Fe_4[Fe(CN)_6]_3\cdot 14H_2O$	3-D	8	$Fe_4[Re_6Se_8(CN)_6]_3\cdot 36H_2O$ (**4**)	
$Ni_3[Fe(CN)_6]_2\cdot 14H_2O$	3-D	14b,d	$Ni_3[Re_6Se_8(CN)_6]_2\cdot 34H_2O$ (**6**)	
$[Mn_2(H_2O)_4][Ru(CN)_6]\cdot 5H_2O$	3-D	47	$[Co_2(H_2O)_4][Re_6S_8(CN)_6]\cdot 10H_2O$	5d
$Na_2Zn_3[Fe(CN)_6]_2\cdot 9H_2O$	3-D	48	$Na_2Zn_3[Re_6Se_8(CN)_6]_2\cdot 24H_2O$	5e
$La[Co(CN)_6]\cdot 18H_2O$	3-D	49		
$Sm[Co(CN)_6]\cdot 18H_2O$	3-D	50		
$Ba_3[Cr(CN)_6]_2\cdot 20H_2O$	3-D	51	$Cs_2[Fe(H_2O)_2]_3[Re_6Se_8(CN)_6]_2\cdot 12H_2O$[b]	5a
$[Zn(H_2O)]_2[Fe(CN)_6]\cdot 0.5H_2O$	2-D	52	$[Zn(H_2O)]_2[Re_6Se_8(CN)_6]\cdot 13H_2O$	5e
$Na_2Cu[Fe(CN)_6]\cdot 10H_2O$	2-D	53	$Cs_2[Mn(H_2O)_2][Re_6S_8(CN)_6]$	5a
$(NMe_4)[Mn(H_2O)_2][Cr(CN)_6]\cdot 2H_2O$	2-D	54	$Cs_2[Mn(H_2O)_2][Re_6S_8(CN)_6]$[b]	5a
$(NMe_4)_2Mn[Mn(H_2O)_2][Cr(CN)_6]_2\cdot 2H_2O$	2-D	55		
$(NMe_4)[Mn(H_2O)_4][Fe(CN)_6]\cdot 4H_2O$	1-D	56	$(NPr_4)_2[Mn(H_2O)_4][Re_6S_8(CN)_6]\cdot 4H_2O$[b]	57

[a] Incorporating octahedral hexacyanometalates. [b] Framework charge differs from that of the metal−cyanide parent.

dantly, the expanded Prussian blue analogues $Co_3[Re_6Se_8(CN)_6]_2\cdot 25H_2O$ (**5**), **6**, and $Ga[Re_6Se_8(CN)_6]\cdot 6H_2O$ (**7**) all behave as simple paramagnets, displaying effective magnetic moments consistent with the combined moments of their individual spin components.

Outlook

The technique of expanding a metal−cyanide framework by replacing its hexacyanometalate units with face-capped octahedral clusters of the type $[Re_6Q_8(CN)_6]^{3-/4-}$ (Q = S, Se) appears to be quite general. Table 4 lists the known structure types incorporating octahedral hexacyanometalate units, and, remarkably, 10 of the 13 variants have now been obtained in expanded form. The high level of control over structure and composition achieved in these systems, should make them attractive candidates for use in tailoring materials to specific applications. In particular, the ability demonstrated here to dehydrate the cubic Prussian blue type solids leaving accessible micropores lined with coordinatively unsaturated metal centers suggests their potential utility as heterogeneous catalysts. Aside from exploring this possibility, future work will focus on applying the technique in the expansion of crystal structures containing metal coordination geometries other than octahedral and bridging ligands other than cyanide.

Acknowledgment. This work was funded by the University of California, Berkeley, the University of California Energy Institute, the Camille and Henry Dreyfus Foundation, and NSF Grant No. CHE-0072691. We thank Prof. P. Yang and Mr. F. Kim for experimental assistance, Dr. A. Mehta for helpful discussions, Prof. A. M. Stacy for use of the X-ray powder diffractometer and SQUID magnetometer, Prof. J. Arnold for use of the thermogravimetric analysis instrument, and Prof. J. M. J. Fréchet for use of the gas sorption analyzer. Segments of the research were carried out at the Stanford Synchrotron Radiation Laboratory and the National Center for Electron Microscopy, which are operated by the Department of Energy, Office of Basic Energy Sciences.

Supporting Information Available: Tables of crystal data, structure solution and refinement, atomic coordinates, bond lengths and angles, and anisotropic thermal parameters for compounds **2**·$3H_2O$, **4**, **6**, **7**, and **8** (PDF); an X-ray crystallographic file (CIF). This material is available free of charge via the Internet at http://pubs.acs.org.

JA0110473

(52) Siebert, V. H.; Nuber, B.; Jentsch, W. *Z. Anorg. Allg. Chem.* **1981**, *474*, 96.
(53) Ayrault, S.; Loos-Neskovic, C.; Fedoroff, M.; Garnier, E.; Jones, D. J. *Talanta* **1995**, *42*, 1581.
(54) Witzel, M.; Babel, D. *Z. Naturforsch.* **1985**, *B40*, 1344.
(55) Witzel, M.; Ziegler, B.; Babel, D. *Z. Anorg. Allg. Chem.* **2000**, *626*, 471.
(56) Henkel, H.; Babel, D. *Z. Naturforsch.* **1984**, *B38*, 880.
(57) Naumov, N. G.; Artemkina, S. B.; Virovets, A. V.; Fedorov, V. E. *J. Solid State Chem.* **2000**, *153*, 195.